Quantifying Inelastic Force and Deformation Demands on Buckling Restrained Braces and Structural System Response

JUSTIN D. MARSHALL, BRANDT SAXEY and ZHONGLIANG XIE

ABSTRACT

Buckling-restrained braced frames (BRBF) have become a very popular lateral-resisting system due to their balanced, full hysteresis and the ability to tailor stiffness, within limits, and strength to meet specific design requirements. This paper reports the results of an analytical investigation on the performance of buckling-restrained braces (BRB) and the global performance of BRBF with a focus on the ductility and overstrength demands on the braces. Nonlinear analytical models of various three- and six-story steel frames were subjected to a suite of earthquake records to determine the demands on the BRB elements and the overall frame response. The structure variations include the location (i.e., seismic hazard), seismic importance factor, I_e, brace configuration (chevron versus single diagonal), and BRB yielding core length. The analysis also investigates the ratio of the impact of an error in the approximation of the BRB elastic stiffness on the system performance.

Keywords: buckling-restrained brace, ductility in steel structures, overstrength demands, nonlinear analysis.

INTRODUCTION

Buckling-restrained braces (BRB) are an example of a recent innovation in structural engineering that has had a significant impact on design of steel structures. As opposed to conventional concentrically braced frames that yield in tension and buckle in compression, BRB have a full and essentially balanced hysteresis. This occurs because the flexural demands are taken by the buckling restraining element of the brace, which allows yielding in tension and compression of the core steel. Yielding in both directions allows for material limit states in both directions and a much greater capacity to dissipate energy than yielding and buckling of a concentric brace. In addition, the geometry of the yielding core plate can be tailored to the strength and stiffness requirements for a given application.

The typical configuration of BRB in U.S. practice today (see Figure 1) consists of a core plate with a yielding region that is tapered down from the connection regions at the end. The core plate is covered by a restraining tube that is filled with mortar to provide the restraining mechanism. Between the steel and mortar, an air gap or bond breaker is used to minimize axial load transfer between the core and the restraining system. Significant experimental and analytical research has investigated the performance of BRB. The original research conducted on a plate debonded from constraining concrete was conducted by Yoshino and Karino (1971) and Wakabayashi et al. (1973). Many researchers since then have investigated a myriad of different combinations of core plate and buckling restraining mechanisms (Xie, 2005; Uang et al., 2004). A significant amount of research has been done related to component testing of BRB; however, system-level research has been less common. A few examples of either experimental or analytical research on system level response include Fahnestock et al. (2006), Mahin et al. (2004), Sabelli (2001), Tsai and Hsiao (2008), and Chou et al. (2012).

One of the challenges in determining the proper ductility-based design requirements for a lateral resisting system is determining appropriate limitations within the code that enable design provisions that result in robust, safe structures. These limitations must then be linked to an elastic design procedure based on an elastic and static analysis model. Currently, BRB are designed and detailed in the United States in accordance with ASCE/SEI 7 (ASCE, 2010) and AISC/ANSI 341 (AISC, 2010a). The provisions that impact BRB design are the seismic performance factors (R, Ω_o, C_d) and the capacity design provisions, which include the tension (ω) and compression (β) strength adjustment factors. The seismic performance factors relate the elastic analysis model to the expected inelastic response. The capacity design requirements ensure that other structural elements in the load path have sufficient capacity for the maximum inelastic demand required of the BRB. The current requirement to determine

Justin D. Marshall, Associate Professor of Civil Engineering, Auburn University, Auburn, AL. Email: jdmarshall@auburn.edu (corresponding)

Brandt Saxey, Vice President Preconstruction Sales and Technical Director, CoreBrace, West Jordan, UT. Email: brandt.saxey@corebrace.com

Zhongliang Xie, Graduate Research Assistant, School of Civil and Construction Engineering, Oregon State University, Corvallis, OR. Email: xiezho@onid.oregonstate.edu

Paper No. 2017-18

the brace forces at the expected deformations requires a drift that is the larger value of 2% of the story height or twice the design story drift. The difficulty with this calculation is that the overstrength (the maximum expected brace force) depends on the geometry of the frame, which can require multiple iterations as section sizes change.

The research aim is to add to the data available on system-level response of BRB. A three-story and a six-story structure, which were previously used for research on braced frames (Sabelli, 2001) and are based on the SAC Steel Project buildings (FEMA, 2000), have been used in this research. The varied parameters include seismic hazard, brace configuration, seismic importance factor (I_e), and yielding core length. Two different seismic hazards—Los Angeles and Riverside, California—are utilized. Both are in the highest seismic design category, but there is a significant difference in the spectral accelerations. Single-diagonal and chevron (inverted-V) configurations are used to evaluate how the yielding core length difference and a reduced number of braces affect performance. The seismic importance factor is investigated by designing the BRB for a normal and critical occupancy structure ($I_e = 1$ and $I_e = 1.5$). Lastly, one of the concerns associated with tailoring BRB for increased stiffness is the impact of a shortened yielding core. Two core lengths using the same cross-sectional area are analyzed to study the impact of excessively short yield lengths. The first yielding core length was associated with the minimal stiffness the brace would be designed for and is referred to as the normal yielding core length. The shorter yielding core length was associated with what was considered the effective maximum stiffness the BRB could achieve. This was established by shortening the yielding core length until a 2% story drift would produce a 3 to 3.5% core strain.

One other component of the study is looking at the importance of accurately modeling the initial stiffness of braces. For typical conventional braces, the brace stiffness is based on the section and the working point lengths. For BRB, significant efforts are made to better approximate the brace stiffness. Using some of the structures in this research, the elastic stiffness was modified by ±10% to determine the impact of initial elastic stiffness on global inelastic response.

STRUCTURE DESCRIPTIONS AND PARAMETERS

All versions of the three- and six-story structures were designed using the equivalent lateral force (ELF) procedure specified in ASCE 7 (2010). The design gravity loads are the same as those specified by Sabelli (2001). The live load for the structures is 50 psf. The structural system is a typical steel frame structure. The basic dead load including superimposed loads varies from about 84 to 89 psf, with the mechanical penthouse having a dead load assigned to the roof of 148 psf. The same gravity system, columns and beams are used for all the versions of the buildings. The only difference among the various building versions is the BRB. A yield stress of 38 ksi was assumed for all BRB designs to size the core areas. The two different seismic hazards used in the analyses are Riverside, CA ($S_{DS} = 1.0$, $S_{D1} = 0.6$), and Los Angeles, CA ($S_{DS} = 1.39$, $S_{D1} = 0.77$). Both locations are considered site class D. The Seismic Design Category for normal occupancy structures is D. For the structures designed with $I_e = 1.5$, the Seismic Design Category is E and F for Riverside and Los Angeles, respectively. In total, 20 building variations were designed; 10 for each height.

Table 1 shows the fundamental period of vibration and the maximum story-drift ratio for each of the 20 building configurations. The model nomenclature, which will be used throughout to identify the structures, is based on the various parameters of the various structures. Los Angeles (LA) and Riverside (Riv) and the number of stories (3 or 6) are the first component. The two letters after the hyphen indicate the brace configuration: either chevron (CH) or single diagonal (SD). The last portion indicates the parameters for increased importance ($I_e = 1.5$) or shortened-yield length (S). Where no final parameter exists following the brace configuration, it represents a normal yield length brace and normal risk category structure ($I_e = 1$). The modal information and maximum story-drift ratios provide information about the stiffness and the dynamics of the various configurations in the elastic realm. The limiting drift ratios for these structures are all within the allowable limit. A 2% drift ratio is the limit for all the structures, with the exception of the structures classified as Risk Category IV ($I_e = 1.5$),

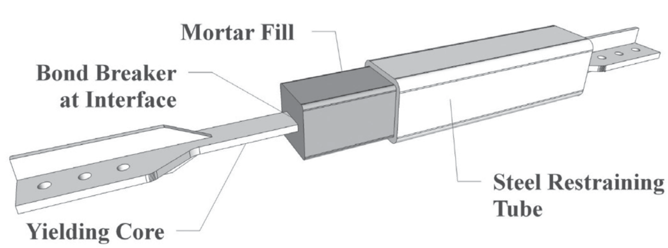

Fig. 1. Typical U.S. BRB configuration.

Table 1. Period of Vibration and Maximum Drift Ratio for Building Models					
Model	Fundamental Period (sec)	Maximum Story-Drift Ratio	Model	Fundamental Period (sec)	Maximum Story-Drift Ratio
LA3-CH	0.52	0.0052	Riv3-CH	0.57	0.0057
LA3-CH1.5	0.45	0.0045	Riv3-CH1.5	0.49	0.0041
LA3-CHS	0.48	0.0051	Riv3-CHS	0.52	0.0046
LA3-SD	0.58	0.0097	Riv3-SD	0.64	0.0089
LA3-SDS	0.49	0.0079	Riv3-SDS	0.53	0.0069
LA6-CH	1.27	0.011	Riv6-CH	1.34	0.010
LA6-CH1.5	1.09	0.009	Riv6-CH1.5	1.18	0.008
LA6-CHS	1.10	0.009	Riv6-CHS	1.16	0.008
LA6-SD	1.44	0.017	Riv6-SD	1.61	0.015
LA6-SDS	1.23	0.014	Riv6-SDS	1.36	0.011

where the allowable drift ratio is 1%. While this information is very valuable for elastic response, the variation in the response of the structure under a nonlinear response history analysis can vary significantly for structures with similar elastic behavior.

Three-Story Structure

The three-story structure is a typical office building with 13-ft story heights. The plan dimensions are 124 ft × 184 ft with 30-ft-square structural bays. The building envelope is 2 ft outside the structural gridlines on all sides. All the braced frames are at the building perimeter. Two bays of bracing are present on each building face. A building elevation and plan are shown in Figure 2. The column and beam sizes are consistent for all the different configurations. Figure 2 shows the chevron bracing in solid lines and the single-diagonal configuration in dashed lines. Table 2 provides details about the BRB elements in all variations of the three-story structures. The yield length ratio is defined as the ratio of the yielding core length to the working point length of the braces.

Six-Story Structure

The six-story structure is also a typical office building. The first story height is 18 ft with the remaining stories having a 13-ft height. The building is square in plan (154 ft) with 30-ft-square bays. The building envelope is 2 ft outside the structural grid. Figure 3 shows an elevation view, and Figure 4 shows a plan view of the six-story structure. Three bays of perimeter bracing are used on each face of the building. Figure 3 shows the chevron bracing in solid lines and the single-diagonal configuration in dashed lines. The fundamental period of vibration and the design story drift for the different configurations of the six-story structure are presented in Table 1. Table 3 shows details about the BRB properties used in the different six-story models. The naming convention for the analysis models is the same as described for the three-story structure.

MODELING AND ANALYSIS

The building designs were completed using SAP 2000 version 15 (CSI, 2013). The nonlinear dynamic analysis was completed in Perform 3D version 5 (CSI, 2011). As is shown in Figures 2 and 3, a planar frame model is used for the analyses. In order to capture P-delta effects, a leaning P-delta column is used. The P-delta column captures the gravity loading and the continuous column effect of the leaning columns. It is a nonstandard column shape with the moment of inertia equal to the sum of the weak-axis properties of the tributary columns. An equal displacement constraint is used at each floor to constrain the P-delta column to the frame. Gravity loads are applied to the model as both point and distributed loads. Distributed loads are used on the beams except where those loads would induce gravity loads into the BRB in the chevron configuration. In this case, the tributary gravity loads were applied directly to the column. Dead load and 50% of live load are applied to the frame before the earthquake analysis. Tributary horizontal joint masses are applied at all the nodes in the model.

Beams in the unbraced bays are modeled as elastic beam elements. Beams in the braced bays, specifically for the chevron configurations, were modeled as inelastic beams based on the potential for plastic deformations due to unbalanced brace forces. A yield stress of 50 ksi was used for the beam elements. All beam column connections were assumed to be pinned connections because it is expected that a simple connection would be used adjacent to the gusset plate to allow for rotation between the beam and column

Table 2. BRB Properties for Three-Story Building Models									
Model	Story Level	Yield Force (kips)	Yield Length (in.)	Yield Length Ratio	Model	Story Level	Yield Force (kips)	Yield Length (in.)	Yield Length Ratio
LA3-CH	3rd	161.5	152.9	0.64	Riv3-CH	3rd	123.5	158.1	0.66
	2nd	247.0	138.5	0.58		2nd	209.0	148.6	0.62
	1st	304.0	131.9	0.55		1st	228.0	138.1	0.58
LA3-CH1.5	3rd	247.0	138.5	0.58	Riv3-CH1.5	3rd	190.0	151.7	0.64
	2nd	380.0	130.1	0.55		2nd	304.0	133.2	0.56
	1st	437.0	127.3	0.53		1st	342.0	130.7	0.55
LA3-CHS	3rd	161.5	67.2	0.28	Riv3-CHS	3rd	123.5	66.6	0.28
	2nd	247.0	66.6	0.28		2nd	209.0	66.9	0.28
	1st	304.0	65.3	0.27		1st	228.0	65.0	0.27
LA3-SD	3rd	266.0	270.1	0.69	Riv3-SD	3rd	209.0	278.4	0.71
	2nd	418.0	258.3	0.66		2nd	342.0	261.8	0.67
	1st	513.0	264.0	0.67		1st	399.0	272.9	0.70
LA3-SDS	3rd	266.0	81.1	0.21	Riv3-SDS	3rd	209.0	81.3	0.21
	2nd	418.0	81.2	0.21		2nd	342.0	80.7	0.21
	1st	513.0	78.4	0.20		1st	399.0	77.9	0.20

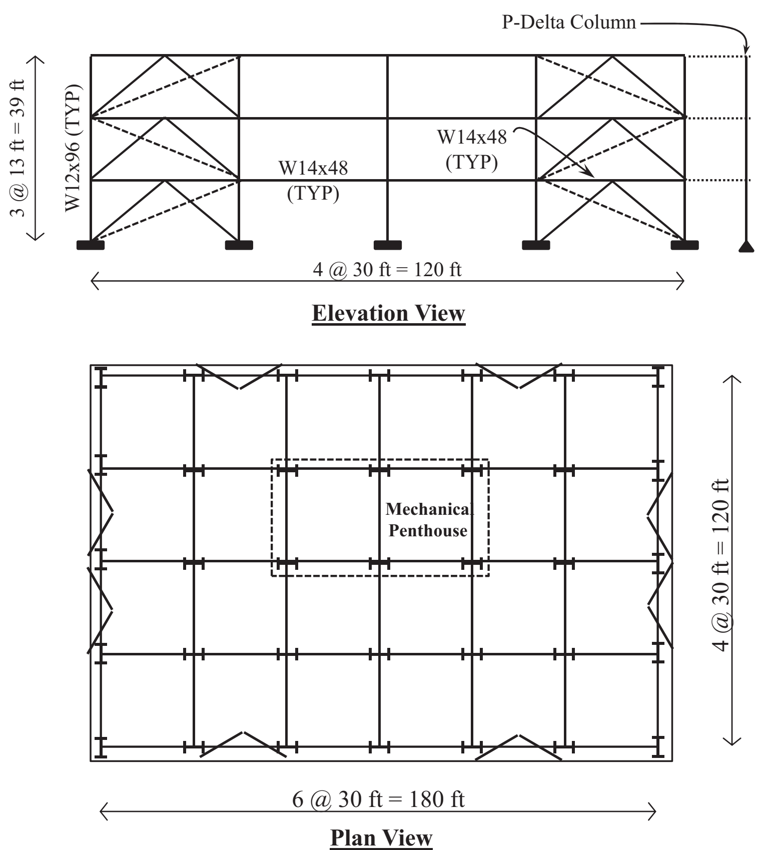

Fig. 2. Elevation and plan view of the three-story structure.

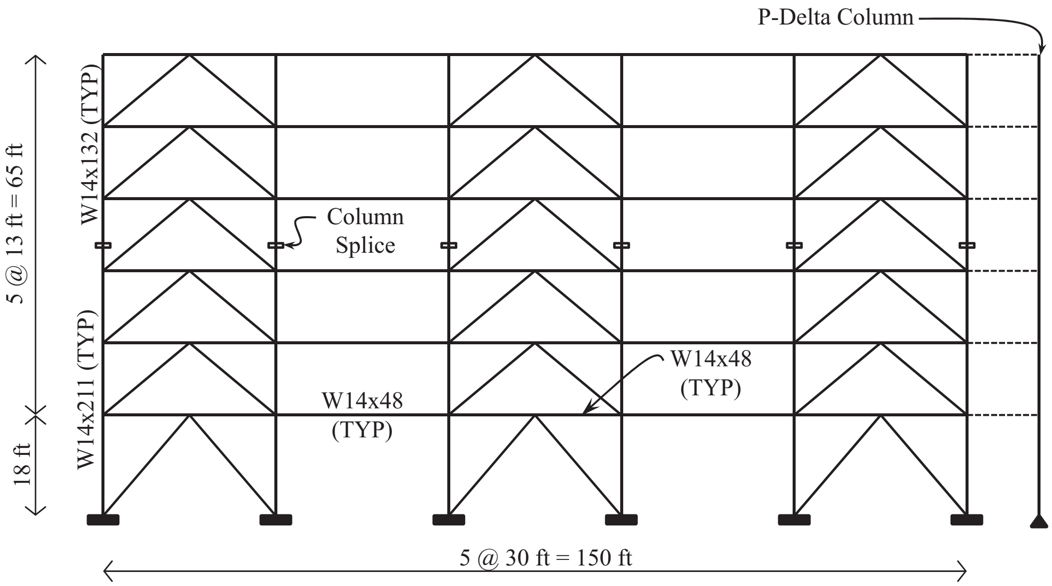

Fig. 3. Elevation view of the six-story structure.

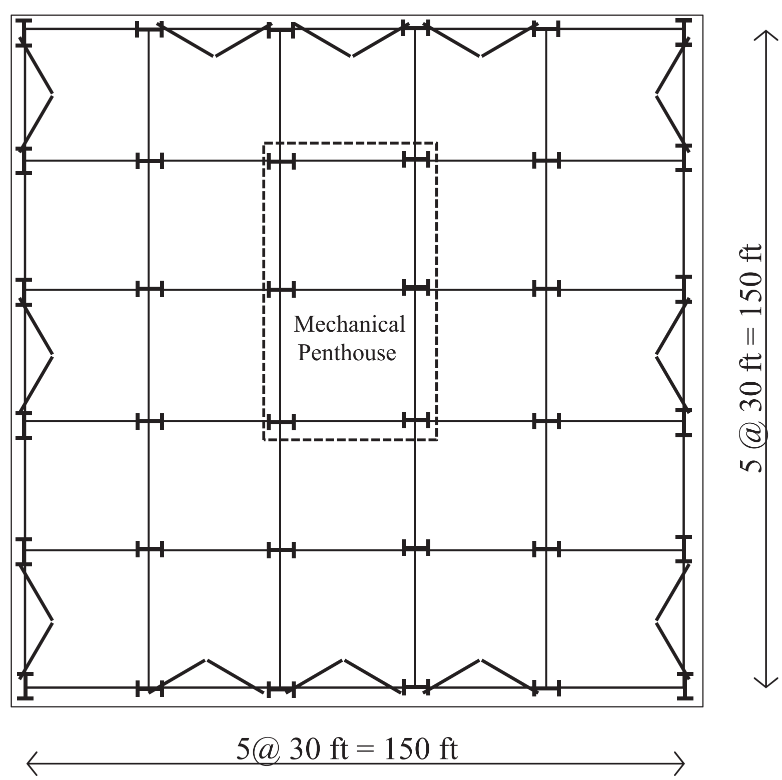

Fig. 4. Plan view of the six-story structure.

Table 3. BRB Properties for Six-Story Building Models									
Model	Story Level	Yield Force (kips)	Yield Length (in.)	Yield Length Ratio	Model	Story Level	Yield Force (kips)	Yield Length (in.)	Yield Length Ratio
LA6-CH	6th	57.0	145.9	0.61	Riv6-CH	6th	47.5	145.2	0.61
	5th	76.0	161.7	0.68		5th	66.5	146.3	0.61
	4th	104.5	146.5	0.62		4th	85.5	145.2	0.61
	3rd	114.0	161.4	0.68		3rd	95.0	144.9	0.61
	2nd	123.5	161.4	0.68		2nd	104.5	144.6	0.61
	1st	133.0	199.7	0.71		1st	114.0	197.5	0.70
LA6-CH1.5	6th	76.0	160.5	0.67	Riv6-CH1.5	6th	66.5	146.3	0.61
	5th	104.5	144.6	0.61		5th	95.0	144.9	0.61
	4th	142.5	156.6	0.66		4th	123.5	158.1	0.66
	3rd	161.5	152.9	0.64		3rd	133.0	157.3	0.66
	2nd	180.5	152.2	0.64		2nd	152.0	153.7	0.65
	1st	190.0	190.4	0.68		1st	152.0	192.3	0.68
LA6-CHS	6th	57.0	67.9	0.29	Riv6-CHS	6th	47.5	67.2	0.28
	5th	76.0	66.5	0.28		5th	66.5	68.3	0.29
	4th	104.5	66.6	0.28		4th	85.5	67.2	0.28
	3rd	114.0	66.8	0.28		3rd	95.0	66.9	0.28
	2nd	123.5	66.1	0.28		2nd	104.5	66.6	0.28
	1st	133.0	78.0	0.28		1st	114.0	79.5	0.28
LA6-SD	6th	76.0	292.0	0.74	Riv6-SD	6th	57.0	277.4	0.71
	5th	114.0	290.1	0.74		5th	95.0	276.2	0.70
	4th	152.0	285.0	0.73		4th	123.5	289.3	0.74
	3rd	180.5	283.2	0.72		3rd	133.0	288.6	0.74
	2nd	190.0	282.7	0.72		2nd	152.0	285.0	0.73
	1st	199.5	327.8	0.78		1st	152.0	329.8	0.79
LA6-SDS	6th	76.0	81.2	0.21	Riv6-SDS	6th	57.0	81.1	0.21
	5th	114.0	81.7	0.21		5th	95.0	81.9	0.21
	4th	152.0	81.2	0.21		4th	123.5	81.9	0.21
	3rd	180.5	81.2	0.21		3rd	133.0	81.8	0.21
	2nd	190.0	81.0	0.21		2nd	152.0	81.9	0.21
	1st	199.5	102.6	0.24		1st	152.0	103.5	0.25

at bracing connections. Columns adjacent to braced bays were modeled to account for possible inelasticity. Columns not adjacent to braced bays were modeled elastically. Modal damping of 2% of critical is used for all the modes. Additionally, a small amount of Rayleigh damping is specified (0.05%) over the range of important periods, which is a recommendation of the Perform 3-D manual (CSI, 2011).

Inelastic modeling of the BRB was completed using the BRB compound element. The compound element includes three primary components. The inelastic component uses the length and cross-sectional area of the BRB core to represent yielding and strain hardening with trilinear behavior and a nonsymmetric backbone curve. The nonsymmetric option allows for the different-strength values of the brace in tension and compression. The elastic bar component models the BRB length outside the core (connection region). The third component, the end zone, is the remaining length between the ends of the brace and the beam-column joint working points. The end zone is established as a multiplier on the elastic bar area. The yield force, initial stiffness, post-yield stiffness, and hardening behavior for the inelastic component as well as the length and equivalent area for the elastic bar component and the end-zone multiplier were provided by CoreBrace LLC.

Two different suites of earthquakes were used. The first suite comes from the SAC ground motion suite for LA with a 2% probability of exceedance in 50 years (SAC, 1994). The SAC motions were only used for the LA models. The second suite is a selection of ground motions from FEMA P695 (2009), including motions from the near- and far-field sets. All ground motions are individually scaled such that the average of the suite is at least 90% of the 2% in 50 years hazard spectrum over the range of interest. The ground motion scale factors are shown in Tables 4 (SAC) and 5 (FEMA P695).

RESULTS AND DISCUSSION OF RESULTS

The reported data include story drift, residual story drift, roof acceleration, normalized brace force (or overstrength), cyclic ductility (or single cycle ductility), reference ductility, brace strain, and cumulative ductility. The story drift represents the maximum drift over the height of the structure. The residual drift is the maximum residual story drift over all stories at the end of the analysis. The roof acceleration is the total roof acceleration. The data reported for braces represent the maximum magnitude that occurred in any brace in tension and compression. To ensure that the maximum response in both directions was obtained, data were taken from braces oriented in both directions. The normalized brace force is the maximum force that occurred in any brace in the structure normalized by the brace tension yield force. This approximately represents the overstrength that would be used in a capacity design procedure.

The three different ductility measures all vary in what they represent. Figure 5 shows a representation of the difference between cyclic and reference ductility. The reference ductility demand is measured from the initial, nonelongated core state. This measure is consistent with ductility demands established in specifications such as ANSI/AISC-341 (AISC, 2010a) and is the ductility demand associated with the reported core strain values. The second measure, cyclic (or single-cycle) ductility demand, reports the largest ductility demand from the negative to the positive (or positive to negative) deformation of a single cycle. For symmetrical loading protocols, the cyclic ductility demand would be equal to twice the reference ductility demand. The cumulative inelastic ductility demand represents the summation of the single-cycle excursions throughout the analysis. The force and displacement data from the brace elements was reduced using subroutines that calculated the cyclic and cumulative ductility. The reference ductility was calculated using the maximum brace deformation in tension and compression.

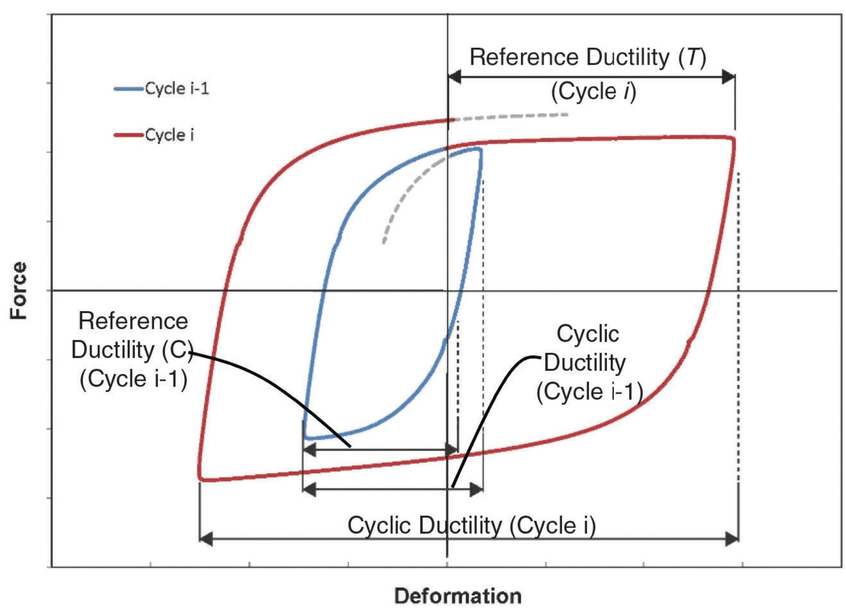

Fig. 5. Schematic representation of ductility demand metrics.

Table 4. SAC Ground Motion Scale Factors					
Ground Motion	LA3	LA6	Ground Motion	LA3	LA6
LA21	0.89	0.85	LA31	0.80	0.91
LA22	1.05	1.04	LA32	0.79	0.85
LA23	2.02	2.05	LA33	1.31	1.20
LA24	1.49	0.99	LA34	1.23	1.17
LA25	1.13	1.02	LA35	1.20	1.08
LA26	1.17	0.88	LA36	1.24	0.91
LA27	1.55	1.48	LA37	N/A	1.10
LA28	0.80	0.85	LA38	N/A	0.93
LA29	1.42	1.43	LA39	N/A	1.57
LA30	1.08	1.05	LA40	N/A	1.29

Table 5. FEMA P695 Ground Motion Scale Factors									
Ground Motion	LA3	Riv3	LA6	Riv6	Ground Motion	LA3	Riv3	LA6	Riv6
FF01-1	2.13	1.49	1.44	1.04	NF09-1	1.14	0.80	0.51	0.58
FF01-2	1.39	0.98	1.46	1.03	NF09-2	1.96	1.38	1.24	1.13
FF02-1	1.91	1.33	3.45	2.47	NF10-1	1.73	1.22	1.40	1.66
FF02-2	2.06	1.45	2.49	2.13	NF10-2	1.13	0.80	0.82	0.82
FF03-1	1.37	0.96	2.05	1.64	NF12-1	2.13	1.86	1.02	0.75
FF03-2	1.65	1.16	1.73	1.43	NF12-2	2.11	1.47	1.14	0.95
FF09-2	2.65	1.86	3.66	2.69	NF15-1	2.16	1.52	1.65	1.31
FF09-2	2.78	1.97	1.67	1.22	NF15-2	1.60	1.13	2.42	1.97
FF16-1	3.42	2.40	3.02	2.19	NF22-1	1.50	1.06	1.43	1.14
FF16-2	4.20	3.00	3.65	2.45	NF22-2	2.26	1.75	2.17	1.74
FF18-1	2.74	1.92	2.46	1.98	NF23-1	1.50	1.05	1.42	1.20
FF18-2	1.43	1.02	2.13	1.72	NF23-2	1.45	1.02	1.65	1.36
FF19-1	3.30	2.88	2.86	2.46	NF24-1	3.22	2.27	3.30	1.90
FF19-2	2.53	1.79	1.77	1.49	NF24-2	1.52	1.07	1.53	1.28
NF02-1	4.20	2.98	2.09	1.69	NF26-1	2.36	1.66	1.46	1.12
NF02-2	2.55	1.79	1.86	1.42	NF26-2	2.08	1.47	1.80	1.34
NF04-1	1.90	1.66	1.05	0.78	NF27-1	0.92	0.81	0.59	0.53
NF04-2	2.72	1.92	2.37	1.66	NF27-2	2.26	1.59	2.06	1.49
NF06-1	2.50	1.75	2.18	1.70	NF28-1	3.36	2.99	1.85	1.34
NF06-2	2.23	1.67	1.32	0.96	NF28-2	2.47	2.16	1.23	0.92
NF07-1	2.14	1.49	2.93	2.50					
NF07-2	1.50	1.04	1.66	1.23					

FF = far field; NF = near field

Table 6. Analysis Results—Los Angeles Three-Story Structure											
Building Model			Story Drift Ratio	Residual Story Drift Ratio	Roof Acceleration (*g*)	Normalized Brace Force	Cyclic Ductility	Reference Ductility	Brace Strain	Cumulative Ductility
P695	LA3-CH	μ	0.036	0.013	1.74	1.92	24.5	23.6	0.031	102.4
		μ+σ	0.051	0.019	2.06	2.21	36.1	34.2	0.045	167.0
	LA3-CH1.5	μ	0.027	0.011	1.86	1.72	18.0	17.9	0.023	67.3
		μ+σ	0.037	0.016	2.25	1.92	26.6	25.3	0.033	102.6
	LA3-CHS	μ	0.026	0.004	1.89	2.40	38.8	32.1	0.042	178.7
		μ+σ	0.035	0.006	2.22	2.84	56.3	44.1	0.058	277.6
	LA3-SD	μ	0.039	0.018	1.60	1.71	15.6	15.4	0.020	64.7
		μ+σ	0.057	0.029	1.89	1.95	22.9	22.7	0.030	103.5
	LA3-SDS	μ	0.025	0.005	2.15	2.34	36.1	29.7	0.039	164.5
		μ+σ	0.034	0.006	2.52	2.75	53.0	41.2	0.054	252.6
SAC	LA3-CH	μ	0.039	0.012	1.90	2.02	29.5	25.7	0.034	110.4
		μ+σ	0.052	0.020	2.12	2.31	46.1	34.8	0.046	147.5
	LA3-CH1.5	μ	0.033	0.013	2.08	1.90	23.8	22.3	0.029	88.0
		μ+σ	0.043	0.019	2.39	2.13	33.4	29.6	0.039	123.2
	LA3-CHS	μ	0.031	0.004	2.11	2.70	47.1	38.5	0.050	204.3
		μ+σ	0.041	0.005	2.37	3.23	68.7	52.5	0.069	265.1
	LA3-SD	μ	0.043	0.019	1.69	1.77	18.4	16.9	0.022	71.9
		μ+σ	0.059	0.031	1.96	2.00	28.6	23.8	0.031	94.6
	LA3-SDS	μ	0.030	0.003	2.25	2.62	43.9	35.1	0.046	194.8
		μ+σ	0.041	0.005	2.50	3.13	64.9	47.9	0.063	258.3
Total	LA3-CH	μ	0.037	0.013	1.78	1.95	25.9	24.2	0.032	104.6
		μ+σ	0.051	0.020	2.09	2.25	39.2	34.4	0.045	163.0
	LA3-CH1.5	μ	0.028	0.011	1.92	1.77	19.6	19.1	0.025	73.1
		μ+σ	0.039	0.017	2.30	1.99	28.9	26.8	0.035	109.5
	LA3-CHS	μ	0.027	0.004	1.95	2.48	41.1	33.9	0.044	185.7
		μ+σ	0.037	0.006	2.28	2.97	60.2	46.8	0.061	276.5
	LA3-SD	μ	0.040	0.018	1.63	1.73	16.4	15.9	0.021	66.7
		μ+σ	0.058	0.030	1.91	1.96	24.7	23.1	0.030	101.9
	LA3-SDS	μ	0.026	0.004	2.18	2.42	38.2	31.2	0.041	172.9
		μ+σ	0.036	0.006	2.53	2.87	56.7	43.3	0.057	256.0

Three-Story Structure

The analysis data are presented in tabular form and include the mean and standard deviation for the suite of earthquakes. Table 6 shows the results from the three-story LA model. The LA data are separated into the SAC and FEMA P695 results. The total results, including both suites combined, are also presented. Table 7 shows the results for the three-story Riverside structure. Table 8 shows the comparison of the results between the various LA and Riverside three-story models. All the results in Table 8 are shown in percentage values. Note that the reference model for the percentage change calculations is indicated in the table. The basis for most of the change calculations is the chevron configuration. However, a supplemental change calculation is provided for the shortened single diagonal as compared to the normal-yield-length single diagonal.

Table 7. Analysis Results—Riverside Three-Story Structure									
Building Model		Story Drift Ratio	Residual Story Drift Ratio	Roof Acceler-ation (g)	Normalized Brace Force	Cyclic Ductility	Reference Ductility	Brace Strain	Cumulative Ductility
Riv3-CH	μ	0.030	0.012	1.16	1.80	21.0	19.6	0.026	85.1
	$\mu+\sigma$	0.044	0.019	1.41	2.14	36.1	33.5	0.044	155.3
Riv3-CH1.5	μ	0.022	0.009	1.31	1.80	14.1	14.1	0.019	52.4
	$\mu+\sigma$	0.032	0.015	1.57	2.14	21.8	21.2	0.028	91.6
Riv3-CHS	μ	0.022	0.005	1.23	2.22	33.2	28.6	0.037	154.1
	$\mu+\sigma$	0.034	0.008	1.46	2.70	53.1	44.2	0.058	272.3
Riv3-SD	μ	0.032	0.015	1.12	1.60	12.6	12.3	0.016	51.0
	$\mu+\sigma$	0.050	0.027	1.33	1.85	20.3	19.3	0.025	90.5
Riv3-SDS	μ	0.022	0.005	1.52	2.15	30.1	25.5	0.033	140.3
	$\mu+\sigma$	0.031	0.007	1.81	2.58	47.4	37.2	0.049	247.8

Table 8. Analysis Result Comparison—LA and Riverside Three-Story Structures Percentage Change in Response Quantities (%)								
Building Model	Story Drift Ratio	Residual Story Drift Ratio	Roof Acceler-ation (g)	Normalized Brace Force	Cyclic Ductility	Reference Ductility	Brace Strain	Cumulative Ductility
LA 3 Story Structures								
Calculation Basis: Model LA3-CH								
LA3-CH1.5	–22.6	–10.1	7.9	–9.3	–24.2	–21.1	–21.1	–30.2
LA3-CHS	–26.1	–66.9	9.6	27.5	58.8	40.1	40.1	77.6
LA3-SD	9.0	46.5	–8.7	–11.3	–36.8	–34.5	–34.5	–36.2
LA3-SDS	–27.	–64.9	22.4	24.1	47.7	29.0	29.0	65.3
Calculation Basis: Model LA3-SD								
LA3-SDS	–33.9	–76.1	34.0	39.8	133.7	96.8	96.8	159.1
Riverside 3 Story Structures								
Calculation Basis: Model Riv3-CH								
Riv3-CH1.5	–25.6	–23.9	12.7	0.0	–33.0	–27.9	–27.9	–38.4
Riv3-CHS	–24.0	–56.5	5.9	23.8	58.4	45.9	45.9	81.1
Riv3-SD	8.7	25.9	–3.9	–10.9	–39.9	–37.1	–37.1	–40.0
Riv3-SDS	–26.9	–58.6	30.8	19.7	43.3	30.2	30.2	64.9
Calculation Basis: Model Riv3-SD								
Riv3-SDS	–32.7	–67.1	36.1	34.4	138.4	106.9	106.9	174.9

These analysis demands are based on maximum credible earthquake (MCE) level, so comparing them to a code-based check at the design level is not a direct comparison. However, based on a simple multiplier, a 2% drift would be scaled by 1.5 to 3%. While nonlinear response cannot be linearly scaled for an individual analysis, this provides a reasonable basis for comparison. Some general comments on the response are that the Riverside drifts are approximately 3%, while the LA maximum drifts are closer to 4%. The design drift ratios presented in Table 1 are generally well below the allowable drift ratios, but the inelastic response is at or above what might be considered an expected MCE response. The code expectation would be that the values would be the same as both structures LA and Riverside are in Seismic Design Category D. With the exception of the shortened braces at the mean plus one standard deviation, the cumulative ductility demands are within the test parameters for buckling-restrained braces in the AISC *Seismic Provisions* (2010a).

The three-story model results indicate several things based on the differences between the two standard brace configurations, chevron and single diagonal. For the typical brace configurations (CH and SD), the single diagonal is more flexible and experiences greater story and residual drifts. The increase in story drifts for the single diagonal compared to the chevron was 9.0 and 8.7% for LA and Riverside, respectively. The increase in residual drift for single diagonal over chevron braces was 46.5 and 25.9% for LA and Riverside, respectively. The trade-off is that the normalized brace force, reference ductility, and cumulative inelastic ductility are lower for the single diagonal. The decrease in normalized brace force in the single diagonal compared to the chevron is approximately 11%. The decrease in the reference ductility demand of single diagonals is 34.5% for LA and 37.1% for Riverside. The decrease in cumulative ductility is 36.2 and 40.0%, respectively, for LA and Riverside. The differences are due to the longer brace yielding length and the longer fundamental period of the single-diagonal structure. The chevron configuration designed with $I_e = 1.5$ results in improved performance in all aspects with the exception of the roof acceleration when compared to the normal risk category design. This increased acceleration is based on the decreased period of vibration.

The shortened brace length (CHS and SDS), which represents an extreme value and may be impractical, has a significant impact on performance. This shortened brace length and the 50% strength increase ($I_e = 1.5$) have a similar impact on the fundamental period of vibration. The reduction in maximum story drifts for the shortened braces ranges from 24 to 34%. The reduction in residual drifts ranges from 57 to 76% for the various three-story models. All other performance metrics result in larger component and system demands when using the shortened yield length. Some metrics change radically. The largest increase is shown in the ductility metrics. The cumulative ductility demand increase for the shortened braces ranges between a 78% increase for the LA chevron up to a 175% increase for the Riverside single diagonal. It should be noted that the relative change in yield length is greater for the single-diagonal configurations, which may be one reason for the larger changes in demands. The reference ductility demand for shortened braces is increased by 46 and 107% for the Riverside chevron and single diagonal, respectively. The increases in reference ductility for LA chevron and single-diagonal shortened braces are 40 and 97%, respectively. The increases in normalized brace force range between 28% for the LA chevron and 40% for the LA single diagonal. Even though the shortened braces experience significantly higher demands, the mean value for cumulative ductility is less than the cumulative demand of 200 from the AISC *Seismic Provisions* qualification protocol. However, the brace demands at mean plus one standard deviation do exceed the qualification test requirement.

Table 9 shows a comparison between the Riverside and the LA three-story response with LA as the basis for the calculation of percentage change. Because the SAC records were not run on the Riverside structure, the most direct comparison of seismic hazard is the FEMA P695 records. The only difference in this case is the scale factor, which is based on the hazard. The biggest difference when looking at the two hazards is the roof acceleration. In all cases, as one would expect, the roof acceleration of the Riverside structures has been reduced to approximately 70% of the value for LA. The other metrics also generally decrease with a few exceptions. It is noteworthy that the metric that had the least impact from the decrease in ground acceleration is the residual drift.

One additional discussion point is the difference between the SAC and FEMA P695 records. The SAC records produce an increased response (higher demands) for everything except the residual drift results. The records for both suites were scaled using the same method to ensure that the mean of the scaled suite did not fall below 90% of the MCE spectrum over the important period range. There is variability in general with ground motion records; however, the SAC records do have a generally higher mean for most of the response quantities reported. As an example, the story drifts under the SAC records increased between 10 and 21%, depending on the structure. The cyclic ductility demand increased from 19 to 32%, and the reference ductility demands increased from 9 to 25%. All these are indicators that this suite of earthquakes is severe and many have large pulses, which have increased certain types of response.

Figure 6 plots brace strain versus normalized brace force for six of the three-story structures. In these plots, the maximum tension and compression value in a first-floor brace are plotted for each record. This provides a better view of

Table 9. Analysis Result Comparison—LA and Riverside Three-Story Structures Percentage Change in Response Quantities (%)								
Building Model	**Story Drift Ratio**	**Residual Story Drift Ratio**	**Roof Acceler-ation (*g*)**	**Normalized Brace Force**	**Cyclic Ductility**	**Reference Ductility**	**Brace Strain**	**Cumulative Ductility**
Calculation Basis: Equivalent LA Model (i.e., Riv3CH/LA3-CH)								
Riv3-CH	–17.3	–5.4	–33.1	–6.3	–14.3	–16.9	–16.9	–16.9
Riv3-CH1.5	–18.2	–14.9	–29.7	4.8	–22.0	–20.9	–20.9	–22.2
Riv3-CHS	–13.2	17.8	–35.0	–7.3	–14.4	–10.9	–10.9	–13.7
Riv3-SD	–17.7	–16.7	–30.3	–6.6	–19.0	–20.1	–20.1	–21.2

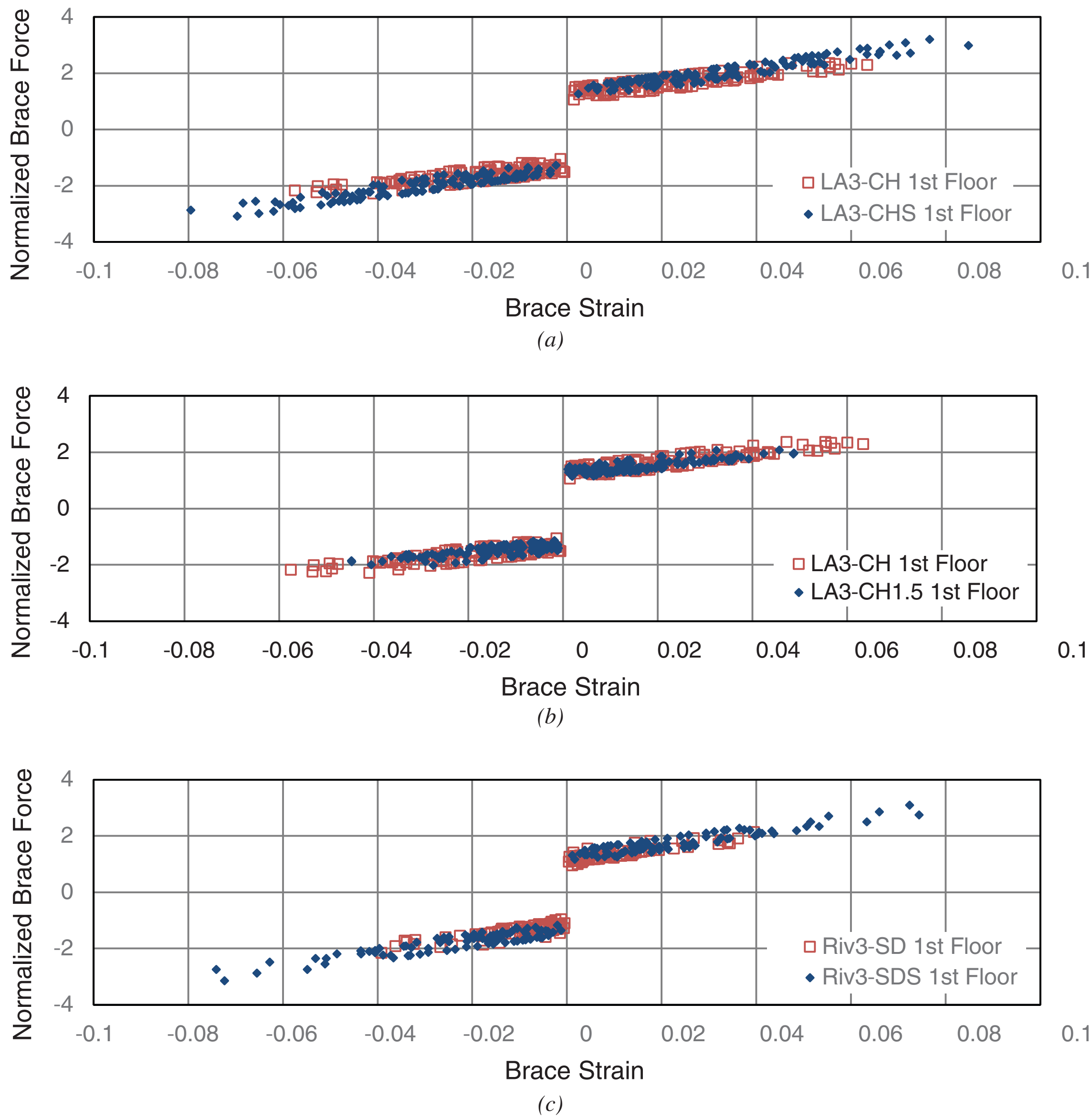

Fig. 6. Brace strain vs. normalized brace force for three-story structures: (a) LA chevron; (b) LA chevron; (c) Riverside single diagonal.

how the data are distributed for the various ground motion records. Figure 6(a) shows the benefits of the importance factor. It is clear that the brace strain is reduced by designing the brace for the higher force demands associated with the higher importance factor. From the Figure 6(b) and 6(c) plots, it can be seen that the shortened-yield-length brace produces a substantial increase in maximum brace force and maximum brace strain. It can also be seen that the single diagonal experiences greater demand increases than the chevron configuration. It should be noted again that these yield lengths are very short, resulting in large normalized brace forces and strains. Some of these strains may be unrealistic in common BRB designs without fracturing the core.

Six-Story Structure

Table 10 shows the analysis results for the LA six-story structures. Table 11 shows the results for the Riverside six-story structures. Table 12 shows the relative percentage change in response quantities for the six-story models using a consistent methodology as was presented previously for the three-story models.

Many similar trends are seen in the six-story results. Just as with the three-story model, a seismic importance factor of 1.5 decreased the story drift by 14% for LA and 18% for Riverside while also decreasing all the ductility metrics by at least 9%. The cumulative ductility demand was decreased by 12 and 9.8% for LA and Riverside, respectively. The shortened-yield-length braces decreased both the story drift and the residual story drift, but in both cases, they increased the ductility measures by at least 107% and by as much as 200%. Again, some of these brace demands are likely not achievable. The normalized force (overstrength) in shortened braces increased by 18% for the chevron and 51% for the single diagonal compared to the equivalent standard-yield-length braces. The percentage increases in demands were greater for the single diagonal as the relative shortening of the single diagonal was much greater.

Table 13 shows a comparison between the Riverside and the LA six-story response with LA as the basis for the calculation of percentage change. As with the three-story, only the P695 ground motions are included in the comparison. The biggest difference when looking at the two hazards is the roof acceleration. In all cases, as one would expect, the roof acceleration of the Riverside structures has been reduced to approximately 77% of the value for LA. This is a smaller reduction in roof acceleration than was seen in the three-story structures. The other metrics also generally decrease, with a few exceptions. One exception is the residual drift. While all the other models showed a decrease of residual drift in Riverside, the chevron had a significant increase (83%) in residual drift, which is unusual. The data for the Riverside residual drift show two of the near-field motions resulting in approximately 5% residual drift and three other near-field records showing greater than 3% residual drift. Utilizing near-field motions for a hazard such as Riverside may be questionable, and the accuracy of residual drifts is also questionable. Due to the lower strength, the Riverside structure was less able to absorb the large energy of a near field record resulting in large drifts and residual drifts.

Figure 7 shows plots of the maximum brace strain and normalized brace force for a selection of the six-story models. The plots in Figures 7(a) and 7(b) show that for both the chevron and single-diagonal configuration, the demands in the upper-story braces are not as large as for the first story, but there is significant inelastic behavior over the height of the structure. For the chevron, the fourth-story brace still experiences greater than 4% strain in several of the quake records, while the first-story brace has several values exceeding 6%. The single diagonal has lower strain levels due to the longer yield length, but the fourth-floor braces experience strains in excess of 2%.

The plot in Figure 7(c) shows the difference between the Risk Category II and IV chevron structures. The differences for the six-story frame are not as significant as for the three-story structure. This is visible in the plot and also shown by the data. Figure 7(d), which has a different scale from the other plots, shows that the effect of the shortened brace is significant for the six-story structure and extends up the building height. Brace strains in excess of 5%, which may not be feasible, result even in the upper floors of the structure.

Table 14 shows a comparison of results for both locations between the different structure heights. The basis of the calculations is the three-story model response. The six-story structures, on average, experienced an increase in maximum story drift over the three-story counterparts. For the LA buildings, the increase ranged from 1.0% for the single diagonal up to 33% for the short-yield-length chevron. The Riverside structure exhibited a 6.3% decrease for the single-diagonal maximum story drift, while all the other configurations increased for the six-story structure by between 9 and 24%. The residual drifts were a more mixed comparison. For LA, the six-story structures had lower residual drifts than the three-story structures for all cases with the exception of the shortened chevron. The residual drift for the six-story shortened-yield chevron structure was nearly double the three-story version. For the six-story Riverside structures, all the residuals decreased from the three-story results with the exception of the chevron, which increased by 45%. The roof accelerations decreased for the six-story buildings for all cases by at least 30% when compared to the three-story buildings. This is expected due to the longer period of vibration.

The metrics representing brace demands also changed from the three- to the six-story buildings. For LA, the normalized brace force increased for all cases of the

Table 10. Analysis Results—Los Angeles Six-Story Structure										
Building Model			Story Drift Ratio	Residual Story Drift Ratio	Roof Acceler-ation (g)	Normal-ized Brace Force	Cyclic Ductility	Reference Ductility	Brace Strain	Cumula-tive Ductility
P695	LA6-CH	μ	0.036	0.009	0.85	1.90	23.0	19.5	0.026	102.4
		μ+σ	0.051	0.016	1.10	2.20	35.5	28.0	0.037	167.0
	LA6-CH1.5	μ	0.031	0.010	0.95	1.82	20.6	17.4	0.023	89.7
		μ+σ	0.043	0.016	1.26	2.06	29.6	24.3	0.032	140.6
	LA6-CHS	μ	0.033	0.008	0.91	2.25	57.5	43.6	0.057	269.3
		μ+σ	0.046	0.013	1.21	2.60	87.3	62.9	0.082	425.4
	LA6-SD	μ	0.035	0.011	0.98	1.74	17.3	14.9	0.020	82.0
		μ+σ	0.051	0.020	1.27	1.99	26.8	21.8	0.029	129.4
	LA6-SDS	μ	0.029	0.004	1.17	2.63	47.4	36.6	0.048	247.5
		μ+σ	0.042	0.007	1.49	3.23	68.8	53.6	0.070	380.7
SAC	LA6-CH	μ	0.048	0.012	0.89	2.14	31.7	26.4	0.035	108.1
		μ+σ	0.068	0.019	1.01	2.45	43.0	36.8	0.048	137.4
	LA6-CH1.5	μ	0.042	0.012	1.06	2.05	29.8	24.3	0.032	96.6
		μ+σ	0.058	0.019	1.25	2.34	41.9	33.3	0.044	121.9
	LA6-CHS	μ	0.044	0.009	0.95	2.50	78.7	58.7	0.077	275.8
		μ+σ	0.060	0.012	1.09	2.88	106.3	81.0	0.106	348.0
	LA6-SD	μ	0.051	0.016	1.03	1.95	24.2	21.4	0.028	82.6
		μ+σ	0.071	0.027	1.16	2.21	33.4	30.0	0.039	103.7
	LA6-SDS	μ	0.042	0.004	1.27	3.20	64.4	52.4	0.069	254.2
		μ+σ	0.062	0.006	1.47	4.01	85.9	77.0	0.101	311.3
Total	LA6-CH	μ	0.040	0.010	0.87	1.98	25.8	21.7	0.028	108.2
		μ+σ	0.058	0.017	1.08	2.30	38.6	31.5	0.041	162.0
	LA6-CH1.5	μ	0.034	0.011	0.99	1.90	23.5	19.6	0.026	91.9
		μ+σ	0.049	0.017	1.27	2.17	34.5	27.9	0.037	136.3
	LA6-CHS	μ	0.036	0.008	0.93	2.33	64.4	48.5	0.064	271.4
		μ+σ	0.052	0.012	1.18	2.71	95.1	70.0	0.092	406.3
	LA6-SD	μ	0.040	0.013	1.00	1.81	19.5	17.0	0.022	82.2
		μ+σ	0.059	0.023	1.25	2.08	29.5	25.1	0.033	123.0
	LA6-SDS	μ	0.034	0.004	1.20	2.81	52.9	41.7	0.055	249.6
		μ+σ	0.050	0.006	1.49	3.54	75.7	62.8	0.082	364.0

Table 11. Analysis Results—Riverside Six-Story Structure									
Building Model		Story Drift Ratio	Residual Story Drift Ratio	Roof Acceleration (g)	Normalized Brace Force	Cyclic Ductility	Reference Ductility	Brace Strain	Cumulative Ductility
Riv6-CH	μ	0.033	0.017	0.640	1.81	19.3	18.0	0.024	84.9
	$\mu+\sigma$	0.048	0.031	0.824	2.10	29.5	26.5	0.035	136.8
Riv6-CH1.5	μ	0.027	0.008	0.729	1.81	17.5	15.2	0.020	76.6
	$\mu+\sigma$	0.037	0.014	0.959	2.10	25.2	20.8	0.027	119.6
Riv6-CHS	μ	0.025	0.005	0.738	2.41	39.8	32.1	0.042	185.7
	$\mu+\sigma$	0.035	0.007	0.974	2.90	58.2	46.2	0.060	290.1
Riv6-SD	μ	0.030	0.010	0.757	1.63	14.1	12.6	0.017	69.9
	$\mu+\sigma$	0.044	0.019	1.004	1.86	22.0	18.5	0.024	113.4
Riv6-SDS	μ	0.026	0.003	0.886	2.29	42.7	32.8	0.043	220.0
	$\mu+\sigma$	0.039	0.005	1.148	2.87	62.7	48.4	0.063	337.1

Table 12. Analysis Result Comparison—LA and Riverside Six-Story Structures Percentage Change in Response Quantities (%)								
Building Model	Story Drift Ratio	Residual Story Drift Ratio	Roof Acceleration (g)	Normalized Brace Force	Cyclic Ductility	Reference Ductility	Brace Strain	Cumulative Ductility
LA Six-Story Structures								
Calculation Basis: Model LA6-CH								
LA6-CH1.5	–14.3	7.9	11.5	–4.2	–10.5	–10.5	–10.5	–12.4
LA6-CHS	–9.3	–13.9	6.8	18.0	150.1	124.3	124.3	163.0
LA6-SD	–1.3	21.4	14.6	–8.6	–25.0	–23.3	–23.3	–19.9
LA6-SDS	–17.8	–58.2	37.2	38.4	106.2	88.2	88.2	141.7
Calculation Basis: Model LA6-SD								
LA6-SDS	–16.7	–65.6	19.7	51.4	174.9	145.3	145.3	201.8
Riverside Six-Story Structures								
Calculation Basis: Model Riv6-CH								
Riv6-CH1.5	–17.8	–51.8	13.9	0.0	–9.0	–15.7	–15.7	–9.8
Riv6-CHS	–26.0	–73.6	15.3	33.2	106.8	78.2	78.2	118.7
Riv6-SD	–9.3	–41.3	18.2	–9.7	–26.8	–30.1	–30.1	–17.7
Riv6-SDS	–20.1	–83.5	38.4	26.6	121.4	81.6	81.6	159.0
Calculation Basis: Model Riv6-SD								
Riv6-SDS	–11.9	–71.8	17.1	40.3	202.2	159.7	159.7	214.9

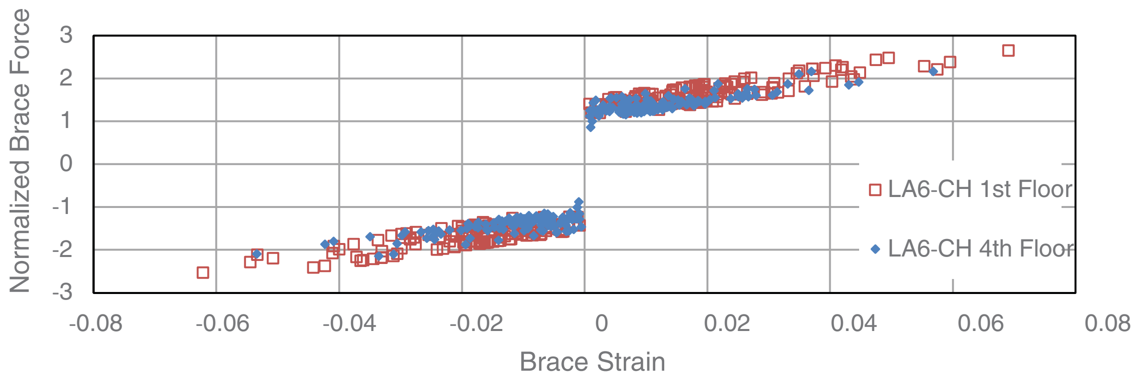

(a)

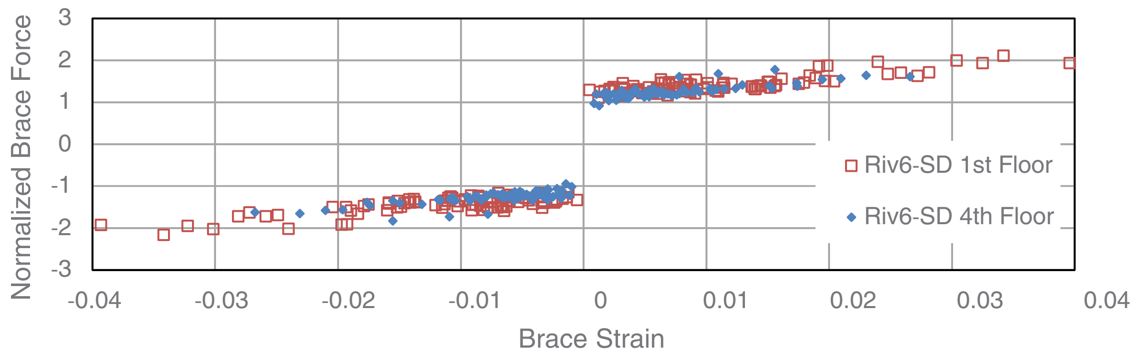

(b)

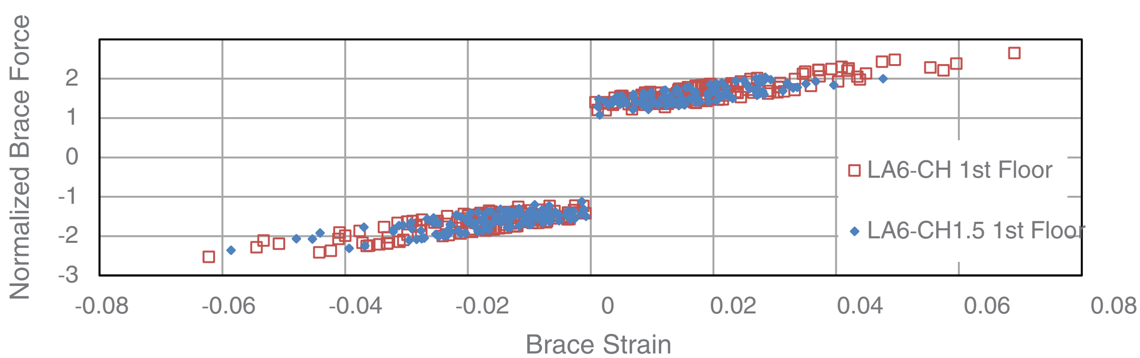

(c)

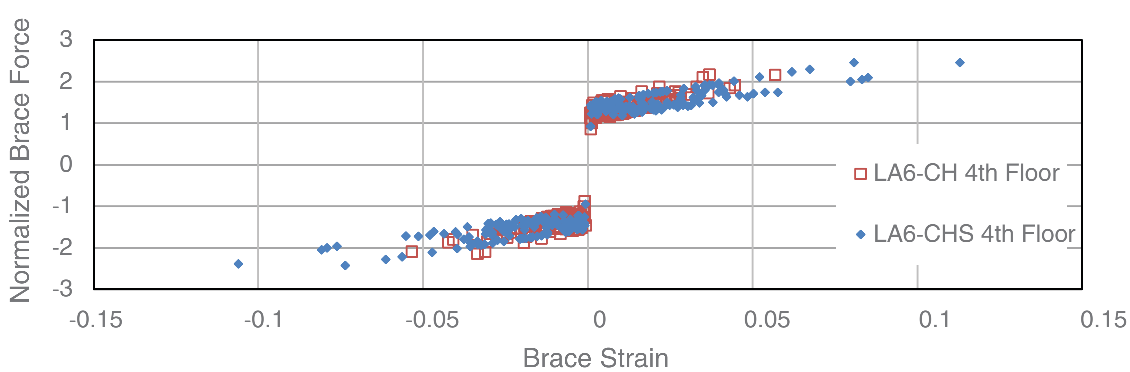

(d)

Fig. 7. Brace strain vs. normalized brace force for six-story structures: (a) LA chevron; (b) Riverside single diagonal; (c) LA chevron and Ι *= 1.5 chevron; (d) LA chevron and shortened chevron.*

Table 13. Analysis Result Comparison—LA and Riverside Six-Story Structures Percentage Change in Response Quantities (%)								
Building Model	Story Drift Ratio	Residual Story Drift Ratio	Roof Acceler-ation (*g*)	Normal-ized Brace Force	Cyclic Ductility	Reference Ductility	Brace Strain	Cumulative Ductility
Calculation Basis: Equivalent LA Model (i.e., Riv6CH/LA6-CH)								
Riv6-CH	–7.6	82.8	–25.0	–4.8	–16.2	–7.3	–7.3	–17.1
Riv6-CH1.5	–11.3	–18.3	–23.4	–0.7	–14.8	–12.7	–12.7	–14.6
Riv6-CHS	–24.6	–43.9	–19.1	7.4	–30.7	–26.4	–26.4	–31.1
Riv6-SD	–15.1	–11.6	–22.7	–6.0	–18.2	–15.5	–15.5	–14.8
Riv6-SDS	–10.2	–27.6	–24.4	–12.9	–10.1	–10.6	–10.6	–11.1

Table 14. Analysis Result Comparison —LA and Riverside Six-Story to Three-Story Structures Percentage Change in Response Quantities (%)								
Building Model	Story Drift Ratio	Residual Story Drift Ratio	Roof Acceler-ation (*g*)	Normal-ized Brace Force	Cyclic Ductility	Reference Ductility	Brace Strain	Cumulative Ductility
LA Structures								
Basis of Calculation: Equivalent LA3 Model (i.e., LA6-CH/LA3-CH)								
LA6-CH	8.8	–17.7	–51.3	1.6	–0.3	–10.3	–10.3	3.4
LA6-CH1.5	21.4	–5.0	–48.6	7.4	20.0	2.9	2.9	25.8
LA6-CHS	33.0	99.4	–52.6	–6.3	56.7	43.2	43.2	46.1
LA6-SD	1.0	–28.9	–38.8	4.5	19.2	7.3	7.3	23.2
LA6-SDS	27.1	–9.1	–44.7	16.5	38.4	33.7	33.7	44.4
Riverside Structures								
Basis of Calculation: Equivalent Riv3 Model (i.e., Riv6-CH/Riv3-CH)								
Riv6-CH	12.3	44.5	–44.9	0.7	–8.1	–8.0	–8.0	–0.2
Riv6-CH1.5	24.1	–8.4	–44.3	0.7	24.7	7.6	7.6	46.2
Riv6-CHS	9.3	–12.2	–40.0	8.4	20.0	12.3	12.3	20.5
Riv6-SD	–6.3	–32.6	–32.2	2.0	11.9	2.3	2.3	36.9
Riv6-SDS	22.7	–42.2	–41.7	6.5	41.9	28.3	28.3	56.8

six-story structure except the shortened yield chevron, which decreased by 6%. The increases ranged from 2 to 16%. An increase in the normalized brace force occurred for all the Riverside six-story configurations. These increases ranged from 1 to 8%. The ductility metrics also generally increased from the three- to the six-story response. The most substantial increases were seen in the shortened yield length configurations. The LA chevron configuration showed the same single-cycle ductility demand and a 10% decrease for the six-story frame in the reference ductility demand and brace strain. The chevron configuration in Riverside showed an 8% decrease from the three- to the six-story building for the single-cycle ductility, reference ductility, and brace strain. The cumulative inelastic ductility demand for the six-story chevron increased by 3% for LA and remained constant for Riverside. The chevron with a 1.5 importance factor and the single diagonal experienced similar trends. Double-digit percentage increases (12 to 46%) for the six-story frame compared to the three-story were seen for the normalized brace force and the cumulative inelastic ductility demand for both LA and Riverside. The reference ductility demand and brace strain increased from 2 to 8% for both brace configurations in both locations. The ductility metrics for the shortened yield length braces all increased by at least 20% for the six-story design. The maximum increases were over 50%, which occurred in the single-cycle ductility demand for the shortened chevron in LA and the cumulative inelastic ductility demand for the Riverside shortened single diagonal.

In general, the performance trends for the different structures behaved as would be expected. The prime example of the deviation was with the residual drifts. The general trends that should be highlighted include the beneficial effect of the importance factor. With the exception of the expected increase in acceleration due to the stiffening effect, all performance metrics were reduced. The effect of the seismic hazard was also interesting as the increase in hazard produced a larger drift demand on the structure. The basis of the code is to maintain the same standard for all structures in a similar Seismic Design Category. The same drift limits and seismic performance factors apply consistently to both structures, but the higher spectral accelerations produced larger demands. Some of this could be attributed to the LA structures having greater stiffness (lower period), which would further increase the accelerations more than just the change spectral accelerations. The shortened-yield-length braces demonstrated the benefit of stiffness in reducing drifts; however, the high cost of maximum brace forces and potentially unobtainable brace strains were particularly troubling.

Cyclic to Reference Ductility Ratio

One other notable aspect is the ratio between cyclic and reference ductility. This is of particular interest because the qualification testing required for BRB in the AISC *Seismic Provisions* (2010a) is based on an increasing-amplitude, symmetric cyclic protocol. This protocol induces a 2:1 ratio between the cyclic and the reference ductility as part of the qualification. The ratios from each record for the LA6-CH are shown in Table 15. In this table, the ratios are broken out by the different subgroups of the ground motion suite. For each of the ground motions, the maximum single-cycle ductility and the reference ductility are shown as well as the ratio of the single cycle to the reference ductility. The average of the three individual subgroups and the overall ground motion suite are shown. The overall average is 1.2. The P695 far-field group has the highest mean of 1.3, while the P695 near-field subgroup has the lowest average at 1.1. This indicates that the far-field events are generally more symmetric than near-field events and result in larger ratios, which are still significantly less than 2. It is interesting to note that in some cases, the ratio is less than 1.0, which indicates that it took multiple smaller cycles to get to the maximum reference inelastic excursion. This is what is sometimes called the ratcheting effect. This indicates that the symmetric loading protocol with a ratio of 2 may not be the best representation of what occurs in a real earthquake event. It also indicates that the maximum inelastic forces, which are based on tests from the symmetric protocol, may not be representative of what occurs in an actual seismic event. Reference strain limits established from symmetric loading protocols are also conservative because they are produced from cyclic strains that are double in value the reference strain. In actual earthquake events, the reference strains will more likely be based on cyclic strains of the same or a similar amplitude. This research indicates that it may be more representative to generate a different testing protocol that is more representative of actual performance. An example of a nonsymmetric, near-fault protocol was recently developed for a BRB in a long-span bridge (Lanning et al., 2016).

BRB Elastic Stiffness Variation

Unlike other structural steel lateral-resisting systems, BRB are generally analyzed to a higher degree to determine the elastic stiffness used in a model. This is done to account for the significant changes in axial rigidity of BRB due to the different cross-sectional properties along the brace length. At some level, this must be done, but a reasonable, simple approximation is likely sufficient. The challenge is that until the design is complete and a BRB manufacturer has provided the geometry, detailed information may not be available, and thus a method for making reasonable approximations is desirable. For concentrically braced frames, the effect of the brace being shortened, the gusset plate, and the beam-column joint are not included in determining the actual brace stiffness, nor is this required by design standards. For reduced beam section (RBS) moment frame connections, the only requirement is that elastic displacements in the model are increased by 10% for flange reductions of up to 50% of the flange width (AISC, 2010b).

In order to investigate the impact of the elastic stiffness on structural response, some of the previous models were run with the elastic stiffness modified by 10% of the value provided by CoreBrace. The models included both a 10% increase and decrease in the stiffness values. The strength values and post-yield behavior remained as they were in the previous analyses. The results of these analyses are presented in Table 16. The entries for the LA6-CH90 indicates the six-story chevron brace with 90% of the CoreBrace provided stiffness, while LA6-CH110 uses 110% of the provided stiffness. The same is true for the single diagonal brace shown. The six-story models of the LA chevron and single diagonal both showed that a 10% change in initial stiffness resulted in maximum changes in response up to 2.7% (residual drift). When looking at the brace demands and the story drift, the maximum change was about 1.3%, indicating that from the perspective of a nonlinear dynamic analysis, the exact

Table 15. Cyclic and Reference Ductility Results—LA Six-Story Chevron

Earthquake Record	Cyclic Ductility	Reference Ductility	Cyclic to Reference Ductility Ratio	Earthquake Record	Cyclic Ductility	Reference Ductility	Cyclic to Reference Ductility Ratio
FF01-1	11.6	14.3	0.8	NF02-1	19.3	17.4	1.1
FF01-2	16.3	11.5	1.4	NF02-2	53.2	45.5	1.2
FF02-1	29.5	25.4	1.2	NF04-1	27.3	18.0	1.5
FF02-2	10.2	9.4	1.1	NF04-2	20.7	20.9	1.0
FF03-1	16.7	16.5	1.0	NF06-1	28.8	19.7	1.5
FF03-2	15.6	12.9	1.2	NF06-2	26.6	27.4	1.0
FF09-1	59.3	36.2	1.6	NF07-1	20.3	20.2	1.0
FF09-2	16.4	16.4	1.0	NF07-2	29.2	33.5	0.9
FF16-1	25.3	23.5	1.1	NF09-1	9.2	9.2	1.0
FF16-2	32.9	23.6	1.4	NF09-2	15.9	11.9	1.3
FF18-1	13.8	9.6	1.4	NF10-1	18.8	16.5	1.1
FF18-2	8.5	6.7	1.3	NF10-2	14.2	13.1	1.1
FF19-1	59.4	37.8	1.6	NF12-1	27.1	18.2	1.5
FF19-2	52.8	31.9	1.7	NF12-2	20.5	16.8	1.2
P695 far-field mean			1.3	NF15-1	10.7	14.0	0.8
P695 far-field mean + standard deviation			1.5	NF15-2	34.9	28.5	1.2
LA21	21.5	15.2	1.4	NF22-1	21.6	23.3	0.9
LA22	21.4	23.4	0.9	NF22-2	18.9	14.0	1.4
LA23	33.9	20.7	1.6	NF23-1	13.0	14.4	0.9
LA24	38.1	34.2	1.1	NF23-2	13.3	10.8	1.2
LA25	23.7	25.4	0.9	NF24-1	14.7	18.3	0.8
LA26	19.9	14.9	1.3	NF24-2	16.6	14.5	1.1
LA27	41.0	32.1	1.3	NF26-1	31.4	33.2	0.9
LA28	21.3	22.1	1.0	NF26-2	16.1	17.5	0.9
LA29	14.7	12.4	1.2	NF27-1	15.5	11.8	1.3
LA30	32.4	26.4	1.2	NF27-2	14.6	19.6	0.7
LA31	19.2	17.4	1.1	NF28-1	22.3	15.0	1.5
LA32	17.9	11.7	1.5	NF28-2	29.2	18.7	1.6
LA33	34.6	24.1	1.4	P695 near-field mean			1.1
LA34	31.5	22.4	1.4	P695 near-field mean + standard deviation			1.4
LA35	54.9	52.7	1.0	Ground motion suite mean			1.2
LA36	49.5	42.2	1.2	Ground motion suite mean + standard deviation			1.4
LA37	38.3	26.7	1.4				
LA38	42.4	28.8	1.5				
LA39	30.5	30.8	1.0				
LA40	50.1	43.9	1.1				
SAC mean			1.2				
SAC mean + standard deviation			1.5				

Table 16. Analysis Results with Initial Stiffness Variation—Los Angeles Six-Story Structure									
Building Model		Story Drift Ratio	Residual Story Drift Ratio	Roof Acceleration (*g*)	Normalized Brace Force	Single Cycle Ductility	Reference Ductility	Brace Strain	Cumulative Ductility
LA6-CH	μ	0.040	0.010	0.87	1.98	25.8	21.7	0.028	108.2
LA6-CH90	μ	0.040	0.011	0.86	1.99	25.7	21.9	0.029	106.6
Percent change		0.65	1.70	–1.09	0.34	–0.56	0.78	0.53	–1.50
LA6-CH110	μ	0.039	0.010	0.88	1.97	25.8	21.4	0.028	108.6
Percent change		–1.05	–2.72	1.76	–0.34	0.11	–1.23	–1.31	0.38
LA6-SD	μ	0.040	0.013	1.00	1.81	19.5	17.0	0.022	82.2
LA6-SD90	μ	0.041	0.013	0.98	1.81	19.4	17.2	0.023	82.2
Percent change		1.28	0.20	–1.71	0.19	–0.69	0.89	0.81	0.03
LA6-SD110	μ	0.040	0.013	1.02	1.80	19.6	16.8	0.022	82.2
Percent change		–1.20	–0.56	2.50	–0.25	0.43	–0.98	–1.22	0.05

stiffness value is not something for which the analysis or the actual response would be highly sensitive. It is important to have a simple approach for engineers to determine a reasonable value for the stiffness of a BRB in an elastic design model without needing a detailed geometry of the brace during the design phase. This is further highlighted by the fact the while the LA3-SD had a design drift of 1.86 times that of LA3-CH, the difference in the nonlinear drift of LA3-SD was only 9% greater than for LA3-CH. Similar trends apply to the other models as well. This is an additional indicator of the fact that while the elastic drifts are important, with all the other assumptions inherent in analyzing structures, a detailed assessment of the BRB stiffness is not required.

SUMMARY AND CONCLUSION

This paper reports on an analytical study on structures with buckling restrained braces using two different seismic hazards and two structure heights coupled with single-diagonal and chevron brace configurations. Several additional parameters were also included to investigate the system performance, brace force, and ductility demands of BRB frames. The 2D nonlinear dynamic analyses were completed with a large suite of earthquakes that included both near-field and far-field records. The important findings and conclusions include:

- The performance of the BRB is within the expected bounds of the code-based limits using the seismic performance factors.
- Many parameters have an influence on the ductility and force demands in BRB, including the brace configuration, importance factor, seismic hazard, and brace yield length. In general, these changes in response follow the expected trends with the primary exception being residual drifts.
- The importance factor has a beneficial effect on brace forces, ductility demands, and story drift. In most cases, it reduces residual drifts, but results in increased roof accelerations as would be expected due to the dynamic properties of the structures.
- The shortened-yield-length braces experienced smaller story and residual story drifts. However, this is coupled with significant increases in acceleration, normalized force demands, and all measures of brace ductility demand. Limits on the yield length of BRB should be considered to avoid the potential for high strains, large forces, or other undesirable effects. Designing to a higher strength may be a better solution if stiffness of the braces needs to be improved. This would result in lower demands in all aspects of the response with the exception of the expected acceleration increase, which would increase with any stiffening of the structure.
- Brace inelastic response was distributed to all levels of the structure with little indication of the potential for developing a soft story due to a single level of braces experiencing all the inelastic response.
- The ratio of the cyclic to reference ductility demand is generally much lower than what results from the symmetric testing protocols for BRB in the AISC *Specification*. This indicates that the forces due to analytical hardening rules determined from testing results may not be consistent with the hardening that occurs due to an actual earthquake. This could have

a potential impact on the expected strength values used as the capacity design elements in BRB system designs.

- The impact of the brace elastic stiffness on the nonlinear response of the models was minimal. The nonlinear analysis demonstrated that structures with significantly different design drift ratios did not have nearly the same difference in inelastic drift ratios. This indicates that assumed brace stiffness values used in design that are sufficiently accurate for elastic models.

REFERENCES

AISC (2010a), *Seismic Provisions for Structural Steel Buildings*, ANSI/AISC-341, American Institute of Steel Construction, Chicago, IL.

AISC (2010b), *Prequalified Connections for Special and Intermediate Steel Moment Frames for Seismic Applications*, American Institute of Steel Construction, Chicago, IL.

ASCE (2010), *Minimum Design Loads for Buildings and Other Structures*, ASCE/SEI 7, American Society of Civil Engineers, Reston, VA.

Chou, C.C., Liu, J.H. and Pham, D.H. (2012), "Steel Buckling-Restrained Braced Frames with Single and Dual Corner Gusset Connections: Seismic Tests and Analyses," *Earthquake Engineering & Structural Dynamics*, pp. 1,137–1,156.

CSI (2011), *User Guide PERFORM-3D: Nonlinear Analysis and Performance Assessment for 3D Structures,* Computers and Structures Inc., Berkeley, CA.

CSI (2013), *CSI Analysis Reference Manual for SAP2000®, ETABS®, SAFE® and CSiBridge®,* Computers and Structures Inc., Berkeley, CA.

Fahnestock, L.A., Sause, R. and Ricles, J.M. (2006), "Analytical and Large-Scale Experimental Studies of Earthquake-Resistant Buckling-Restrained Braced Frame Systems," ATLSS Report No. 06-01.

FEMA (2000), *State of the Art Report on Systems Performance of Steel Moment Frames Subject to Earthquake Ground Shaking,* Federal Emergency Management Agency, Washington DC.

FEMA (2009), *Quantification of Building Seismic Performance Factors,* Report No. FEMA-P695, Applied Technology Council, Redwood City, CA.

Lanning, J., Benzoni, G. and Uang, C.-M. (2016), "Using Buckling-Restrained Braces on Long-Span Bridges I: Full Scale Testing and Design Implications," *Journal of Bridge Engineering*, Vol. 21, No. 5, doi: 10.1061/(ASCE)BE.1943-5592.0000781, 04016001.

Mahin, S., Uriz, P., Aiken, I., Field, C. and Ko, E. (2004), "Seismic Performance of Buckling Restrained Braced Frame Systems," *Proceedings 13th World Conference on Earthquake Engineering,* Vancouver, B.C., Canada, p. 1681.

Sabelli, R. (2001), "Research on Improving the Design and Analysis of Earthquake-Resistant Steel-Braced Frames," Earthquake Engineering Research Institute, Oakland, CA.

SAC (1994), "Suites of Earthquake Ground Motions for Analysis of Steel Moment Frame Structures," retrieved from http://nisee.berkeley.edu/data/strong_motion/sacsteel/ground_motions.html.

Tsai, K.C. and Hsiao, P.C. (2008), "Pseudo-Dynamic Test of a Full-Scale CFT/BRB Frame—Part II: Seismic Performance of Buckling-Restrained Braces and Connections," *Earthquake Engineering & Structural Dynamics*, Vol. 37, No. 7, pp. 1,099–1,115.

Uang, C.M., Nakashima, M. and Tsai, K.C. (2004), "Research and Application of Buckling Restrained Braced Frames," *International Journal of Steel Structures,* Vol. 4, No. 4, pp. 301–313.

Wakabayashi, M., Nakamura, T., Katagihara, A., Yogoyama, H. and Morisono, T. (1973), "Experimental Study on Elastic Plastic Hysteric Behavior of Flat Bar Braces Encased by in Concrete Wall without Bound, Part 1, Preliminary," *Proceedings of the Annual Convention of the Kinki Section of the Architectural Institute of Japan*, pp. 121–144.

Xie, Q. (2005), "State of the Art of Buckling-Restrained Braces in Asia," *Journal of Constructional Steel Research*, Vol. 61, No. 6, pp. 727–748.

Yoshino, T. and Karino, Y. (1971), "Experimental Study on Shear Wall with Braces: Part 2," *Summaries of Technical Papers of Annual Meeting,* Architectural Institute of Japan, Structural Engineering Section, pp. 403–404.